Spectrally resolved bioluminescence optical tomography

Hamid Dehghani,* Scott C. Davis, Shudong Jiang, Brian W. Pogue, and Keith D. Paulsen

Thayer School of Engineering, Dartmouth College, 8000 Cummings Hall, Hanover, New Hampshire 03755

Michael S. Patterson

Juravinski Cancer Centre and McMaster University, Hamilton, Ontario, Canada

Received August 16, 2005; revised October 13, 2005; accepted October 22, 2005

Spectrally resolved bioluminescence optical tomography is an approach to recover images of luciferase activity within a volume using multiwavelength emission data from internal bioluminescence sources. The underlying problem of uniqueness associated with nonspectrally resolved intensity-based bioluminescence tomography is highlighted. Reconstructed images of bioluminescence are presented by using as input both simulated and real multiwavelength data from a tissue-simulating phantom. The location of the internal bioluminescence is obtained with 1 mm accuracy. Further, the amplitude of the reconstructed source is proportional to the actual bioluminescence intensity. © 2006 Optical Society of America

OCIS codes: 110.6960, 100.3010.

Bioluminescence optical tomography (BLT) is an emerging imaging technique where the molecular luminescence from luciferase is used to reconstruct its spatial distribution and to visualize function, physiology, or genetic activation within tissue. The light emitted by luciferase can be detected at discrete locations on the tissue surface by using either contact (e.g., optical fibers) or noncontact approaches (e.g., a CCD camera). A measured set of emission data forms the basis for tomographic reconstruction of the internal bioluminescence distribution analogous to positron emission tomography (PET) by using the mathematics familiar to near infrared (NIR) transmission optical tomography. This Letter demonstrates that multiwavelength or spectrally resolved bioluminescence tomography (sBLT) is essential for direct depth-resolved recovery of the bioluminescence target distribution.

In vivo bioluminescence imaging involves cells that are tagged with a reporter gene that encodes the sequence for the light-generating enzyme Luciferase. Luciferase is produced by the cell and is a protein that can generate visible light through the oxidation of an enzyme-specific substrate. This process requires the presence of oxygen and ATP as a source of energy, and part of the chemical energy is released as visible light, which becomes an optical signal of cellular activity *in vivo*. The background is inherently low since endogenous light from mammalian cells is essentially zero. Luciferase has therefore become a frequently used reporter in many biochemical and cell culture assays. Tumor metastases studies,[1] wound healing imaging,[2] and immune trafficking[3] are some examples of luciferase imaging under investigation. As these studies progress, it is imperative to have improved imaging methods to visualize and quantify the bioluminescence signals *in vivo* in order to gain new insights into tumor growth, regression, immune response, and cellular response to therapy.

Recent interest in modeling and reconstruction algorithms for BLT has increased[4,5] and led to the general consensus that nonspectrally resolved intensity-based BLT results in a nonunique problem.[6] However, the emitted light from firefly luciferase is widely distributed over the band of wavelengths from 500 to 650 nm and above. When not attenuated, it has a peak emission near 560 nm, but when detected from within an animal, it appears to have a peak closer to 600 nm with measurable emissions as much as 50 nm above and below this peak.[7] Using current technology it would be possible to measure the emission at the surface of the tissue in discrete steps of 10 nm ranging from 550 to 650 nm.

This Letter demonstrates the algorithm developments necessary for multiwavelength BLT image reconstruction. It is demonstrated through reconstructed images from simulated noisy data and phantom measurements that recovery with single-wavelength BLT is nonunique whereas multiwavelength sBLT produces images that are not only spatially accurate but also recover source strength proportional to true source intensity.

The mathematical basis for sBLT is the Boltzmann transport equation, and under the assumption that scattering dominates absorption for red light in tissue, the Boltzmann transport equation can be simplified to the diffusion approximation, which for a continuous light source is given by

$$-\nabla \cdot D(\mathbf{r}) \nabla \Phi(\mathbf{r}) + \mu_a \Phi(\mathbf{r}) = B(\mathbf{r}), \tag{1}$$

where $B(\mathbf{r})$ is an internal bioluminescence source, $\Phi(\mathbf{r})$ is the photon fluence rate at position $\mathbf{r}$, $D = 1/3(\mu_a + \mu_s')$ is the diffusion coefficient, μ_a is the optical absorption coefficient, and μ_s' is the reduced scatter coefficient. A Robin boundary condition is used to account for reflection and refraction at the tissue surface. The fluence rate data can be represented by an operator, which is linear in terms of the bioluminescence source. It is assumed that absorption and scatter are known from separate measurements and reconstructions.[8] Thus the BLT image reconstruction problem is posed as a solution to the minimization:

0146-9592/06/030365-3/$15.00

$$\hat{\chi} = \arg\min_{\mu_a,\kappa} \|(\mathbf{y} - F[B(r)])\|, \quad (2)$$

where y is the measured data, $F[B(r)]$ is the data calculated using Eq. (1) given an estimate of the internal bioluminescence distribution model, and $\| \|$ is the weighted L2 norm, representing the square root of the sum of the squared elements. If the location of the bioluminescence source $B(\mathbf{r})$ is known *a priori*, one can constrain the problem to calculate the strength of $B(\mathbf{r})$ to minimize $\hat{\chi}$ in Eq. (2). However, if no prior information about $B(\mathbf{r})$ is available, the problem is inherently more difficult, since both the source strength and its spatial distribution may vary. Fortunately, the photon fluence rate, which is the measured observable, is linear in $B(r)$; hence a practical approach to solving this problem constructs the image of the bioluminescence source as a sum of basis distributions whose weights are estimated from the measured response. Thus we take advantage of the linearity of the model by creating a set of independent basis solutions for the source, $B = \Sigma_{i=1}^{N} a_i b_i$, where the coefficients a_i are the weight functions for multiple unit sources b_i at each node i in the model containing a total number of nodes N. The size of B is reduced if a coarser basis is used for the source relative to the discretization of Φ in Eq. (1). Substituting this matrix expression into Eq. (2) and solving for a in a least-squares manner results in a single-step linear expression, $a = W^{\mathrm{T}}(WW^{\mathrm{T}} + \lambda I)^{-1} y$, where $\mathbf{W}$ is a matrix containing the solution of Eq. (1) for all possible source positions N and y is the measured boundary flux. Here λ is a regularization parameter and I is the identity matrix. Although the Hessian matrix WW^{T} is invertible, the use of λ becomes necessary in the presence of noise in the data. In this work, $\lambda = 0.001\%$ of the maximum of the diagonal of the Hessian.

The 2D circle shown in Fig. 1(a) of radius 20 mm represents soft tissue containing 20 μm of total blood with 75% oxygen saturation and 60% water. Both the scatter amplitude and power of the tissue were assumed to be unity. The corresponding optical properties for a range of wavelengths from 600 to 650 nm

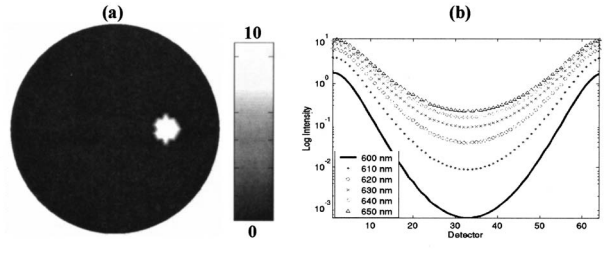

(c)

	λ = 600 nm	λ = 610 nm	λ = 620 nm	λ = 630 nm	λ = 640 nm	λ = 650 nm
μ_a (mm^{-1})	0.0281	0.0162	0.0109	0.0082	0.0067	0.0058
μ_s` (mm^{-1})	1.6667	1.6393	1.6129	1.5873	1.5625	1.5385

Fig. 1. (a) Schematic of the 2D bioluminescence model of 20 mm radius used to generate simulated data. (b) Boundary bioluminescence data generated for each wavelength by using the optical properties as shown in (c).

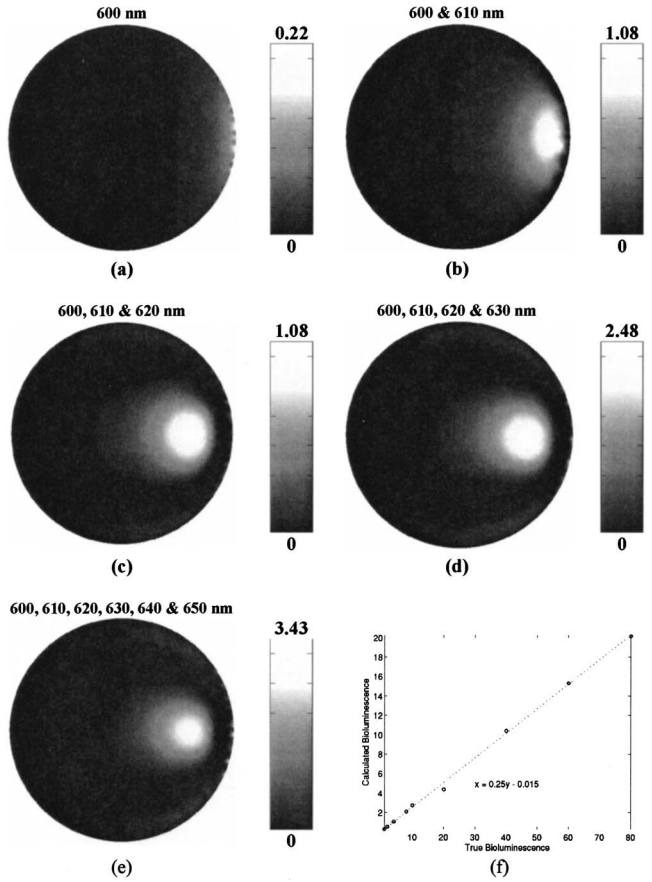

Fig. 2. Reconstructed images of bioluminescence using (a) single and (b)–(e) multiwavelength noisy data. (f) Plot of calculated bioluminescence values versus true strength.

are tabulated in Fig. 1(c) and were used to generate the boundary data presented in Fig. 1(b) for a single bioluminescence source of 5 mm diameter and relative strength 10 placed 10 mm from center as shown in Fig. 1(a). The boundary data from 64 detector positions spaced equally around the external periphery of the model vary significantly with wavelength, reflecting the spectral dependence of the tissue optical properties.

To illustrate the nonuniqueness of the BLT image reconstruction problem, each data set in Fig. 1(b) was individually corrupted with 1% Gaussian noise and used to generate images of the internal bioluminescence distribution. Figure 2(a) shows a typical result for 600 nm, where it is evident that the source is recovered as a very superficial blur along the boundary. Images reconstructed for the other individual wavelengths exhibit similar characteristics.

Instead of using data from a single wavelength, multiwavelength sBLT combines data sets that are measured from the same domain containing the same bioluminescence distribution over a range of usable wavelengths such that $a = \tilde{W}^{\mathrm{T}}(\tilde{W}\tilde{W}^{\mathrm{T}} + \lambda I)^{-1}\tilde{y}$, where $\tilde{W} = [W_{\lambda 1}; W_{\lambda 2}; W_{\lambda 3}; \ldots; W_{\lambda n}]$ are the weight matrices of all n of cascaded wavelengths and $\tilde{y} = [y_{\lambda 1}; y_{\lambda 2}; y_{\lambda 3}; \ldots; y_{\lambda n}]$ is the corresponding measured boundary data for each wavelength. The solution a is a vector corresponding to the number of unknowns that define the bioluminescence source distribution.

Representative images are reconstructed using combinations of two, three, four, or six wavelength data sets (corrupted with noise) over the 600–650 nm wavelength band as shown in Figs. 2(b)–2(e). The use of as few as two sets of wavelengths dramatically improves the accuracy of the reconstructed image. Incorporating additional data sets improves both the quantitative and qualitative accuracy of the reconstructed images. The location of the reconstructed source for the six wavelength band case is within 1 mm of the original target location.

To demonstrate the linearity of the reconstructed bioluminescence versus its true strength, sets of boundary data were generated for the 2D model in Fig. 1(a), where the relative bioluminescent source strength was varied from 1 to 80. Images were reconstructed from the six wavelengths of data ranging from 600 to 650 nm. The maximum reconstructed value of bioluminescence versus the actual value is plotted in Fig. 2(f). As expected, there is a strong linear relationship between the actual and reconstructed bioluminescence values, which is important when one is investigating physiological or functional changes as a function of time.

Finally, to validate the method by using experimental data, measurements were recorded for a single bioluminescence source placed within an otherwise uniform cylindrical phantom of 50.8 mm diameter. The phantom was filled with a solution of 0.2% intralipid and 0.2% oxygenated blood. The bioluminescent source was a 50:50 mixture of 165 micromolar ATP solution with luciferase reagent solution solubolized in 1 ml distilled water (CLS II Kit, Roche Diagnostics, Inc.). The solution was held in a plastic cylinder of 5 mm diameter, placed 7 mm inside the edge at the 3 o'clock position. Sixteen equally spaced measurements around the periphery were collected sequentially using a 1 mm silica fiber bundle leading to a single line of 200 μm fibers entering a spectrometer (Acton SpectraPro 2300i spectrometer with a 300 line/mm grating blazed at 750 nm wavelength) coupled to a cooled CCD (Princeton Instruments Spec-10 XTE CCD). Integration time was 15 min per sample, and a fresh sample was used for each detector location to avoid the effect of source decay. The measured spectrum of the bioluminescence source was normalized using an unattenuated emission spectrum from a dilute sample. An image of the bioluminescence source was reconstructed and is shown in Fig. 3. This image was based on five wavelength intervals of 10 nm, ranging from 600 to 650 nm. Over this range the absorption coefficient varied from 0.0009 to 0.0043 mm^{-1} and the reduced scattering varied from 0.34 to 0.4 mm^{-1} across the wavelengths used. These background optical properties are easily obtained for a complex system by using spectral reconstruction at NIR wavelengths as discussed elsewhere.[8] As is evident in Fig. 3, the image reconstructed by using multiwavelength data has accurately estimated the size and location of the internal bioluminescence source at approximately 7.5 mm from the surface with a full width at half maximum of 8 mm, despite the relatively coarse spatial sampling of the emission. Instrumentation improvements, such as more boundary data and improved signal quality, are expected to improve the quality of images.

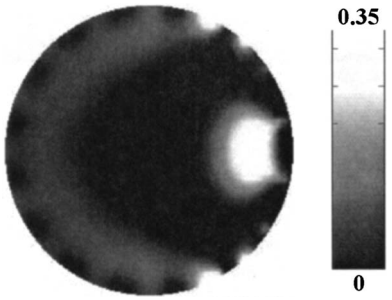

Fig. 3. Reconstructed image of bioluminescence by using multiwavelength measured phantom data.

In this Letter a modeling and linear single step image reconstruction algorithm for sBLT is presented that demonstrates for the first time, to our knowledge, BLT image recovery from experimental multiwavelength data. Multiwavelength emission provides a means of estimating the depth of an object due to the wavelength-dependent attenuation of tissue. Images generated from both noisy simulated data and measured experimental data have been presented. The reconstructed images of bioluminescence are linear with respect to the original target source strength, which is important when using the magnitude of the bioluminescence intensity to quantify physiological function, disease progression, or response to intervention. Certain challenges remain that are the subject of further study, including reconstruction of the unknown absorption and scattering properties and the design and improvement of instrumentation that will allow the simultaneous detection of the bioluminescence spectrum with an optimum signal-to-noise ratio.

This work has been funded by U.S. Department of Defense grants DAMD17-03-1-0405, PO1CA80139, and RO1CA109558.

*Present address, School of Physics, University of Exeter, Exeter UK.

References

1. C. H. Contag and B. D. Ross, J. Magn. Reson Imaging **16**, 378 (2002).
2. M. R. Hamblin, D. A. O'Donnell, N. Murthy, C. H. Contag, and T. Hasan, Photochem. Photobiol. **75**, 51 (2002).
3. J. Hardy, M. Edinger, M. H. Bachmann, R. S. Negrin, C. G. Fathman, and C. H. Contag, Exp. Hematol. **29**, 1353 (2001).
4. G. Alexandrakis, F. R. Rannou, and A. F. Chatziioannou, Phys. Med. Biol. **50**, 4225 (2005).
5. X. Gu, Q. Zhang, L. Larcom, and H. Jiang, Opt. Express **12**, 3996 (2004).
6. G. Wang, Y. Li, and M. Jiang, Med. Phys. **31**, 2289 (2004).
7. C. H. Contag and M. H. Bachmann, Annu. Rev. Biomed. Eng. **4**, 235 (2002).
8. S. Srinivasan, B. W. Pogue, S. Jiang, H. Dehghani, and K. D. Paulsen, Appl. Opt. **44**, 1858 (2003).